



# UNIFIED STRAIN-BASED PROCEDURE TO OBTAIN DESIGN *P-M* INTERACTION CURVES OF SLENDER RC WALL SECTIONS

Aditya Deshmukh <sup>(1)</sup>, Rupen Goswami <sup>(2)</sup>

<sup>(1)</sup> M.S. Student, Department of Civil Engineering, Indian Institute of Technology Madras, India  
E-mail: adityadeshmukh456@gmail.com

<sup>(2)</sup> Assistant Professor, Department of Civil Engineering, Indian Institute of Technology Madras, India  
E-mail: rg@iitm.ac.in

## Abstract

Reinforced concrete structural walls, suitably located in plan, function as the main lateral load resisting elements in buildings. Rectangular and flanged cross-sections are traditionally adopted in practice, depending on functional and architectural requirements of buildings; for instance, C-shaped walls are used as single elevator core in buildings, L-shaped walls at corners of buildings, and T-shaped walls at the periphery of buildings. Axial force – bending moment (*P-M*) interaction diagram is required of these wall sections for design of relatively slender walls. But, generation of design *P-M* interaction curve is iterative, and thus, computationally expensive. The paper presents a simple unified strain-based procedure to obtain design *P-M* interaction curves of both rectangular and flanged RC wall cross-sections. The proposed non-iterative procedure provides closed-form expressions that satisfies compatibility of normal strains, equilibrium of forces, and uses design constitutive relations of the materials. The results obtained compare well with those using traditional nonlinear analyses.

Keywords: *shear wall, barbell wall, limit-state design*

## 1. Introduction

Structural walls are highly efficient in resisting in-plane loads, owing to large in-plane stiffness and strength. However, their behavior depends on design including elevation aspect ratio, cross-sectional shape and location within the plan of a building. In practice, RC rectangular and flanged walls (of I, C, and T shapes) are frequently used. They are designed to resist in-plane loads through shear (truss action) and flexure (cantilever action). However, in case of slender walls, flexural strength, which is a function of axial force, governs the design. Thus, relatively slender structural walls are generally designed considering axial force – bending moment (*P-M*) interaction. Since more than one load combination may have to be considered in design, it is advantageous to construct the design *P-M* interaction capacity diagram to ensure that the combination of axial load and bending moment demand corresponding to the design load combinations are within the interaction diagram. Design handbooks, e.g., SP 16:1980, SP-17(14) [1, 2], provide design *P-M* interaction charts of shallow rectangular and circular RC column sections. Because of variability of wall section shapes, standard *P-M* interaction charts for wall sections are not readily available. As a consequence, designers usually estimate flexural strength from first principles. Multi-layer arrangement of reinforcement and usual complexity of section shape increase computational effort in section analysis for flexural strength, with or without axial load. Thus, design codes, e.g., ACI 318-83 [3], provide expressions for flexural strength of RC rectangular wall sections for given axial load. In addition, uniform distribution of reinforcement is often assumed (e.g., IS13920-1993 [4]). For walls of any other shape, design codes (e.g., ACI 318-14 [5], NZS 3101 [6], Eurocode 8 [7]) usually recommend section analysis, based on condition of equilibrium of forces and compatibility of strains using plane section hypothesis. This lead to some analytical studies that vary depth of neutral axis from zero to a maximum depth equal to length of wall and beyond, to obtain the interaction [8, 9]. Interaction curves obtained using codal expressions or section analysis are also available [9, 10]. However, they are limited to specific limit states and wall geometric configuration. Similar *P-M* interaction is considered in column design too, wherein it is sufficient to calculate flexural strength at only eight different levels of axial loads, to obtain entire interaction curve [11]. There is a need to develop consistent approach to obtain design *P-M* interaction diagrams of RC wall sections of commonly used cross-sectional shapes, using basic principles of mechanics, considering equilibrium of forces, compatibility of strains, and design constitutive relations of constituent materials.



## 2. Methodology

Listed below are the steps followed in the methodology adopted, to obtain design  $P$ - $M$  interaction curve of a given shape of RC wall section:

- i. Specific points on the interaction curve are selected at which the strain profiles are unique and known *a priori*. Selection of number of points depends on geometry of cross-section; 5 points for rectangular wall, 7 points for walls with I and C cross-section shapes, and 6 points for walls with T cross-section shape, are sufficient;
- ii. At each select point, strain at extreme concrete edges and each reinforcing bar level in the cross-section is determined using the unique strain profile;
- iii. At each select point, stress profile in the cross-section is obtained using the design constitutive relations of the materials;
- iv. At each select point, the  $P$  and  $M$  on the design  $P$ - $M$  envelope are determined using closed-form equations of equilibrium;
- v. For each select point, steps ii-iv are repeated; and
- vi. Coordinates ( $M$ ,  $P$ ) of the select points are joined, to obtain the desired design  $P$ - $M$  interaction curve.

### 2.1 Assumptions

To use the above methodology, following assumptions are made:

- i. Plane sections normal to longitudinal axis of member remains plane after bending, allowing use of linear strain profile across the cross-section, such that the strain at any level in the cross-section is directly proportional to the distance from the neutral axis to the considered level;
- ii. Design limiting strain in concrete in compression is 0.0035 (this is as per Indian Standard 456 [12], as discussed in 2.2; in general, any value recommended by corresponding design standard is equally applicable);
- iii. Concrete has zero tensile strength;
- iv. Design limiting strain in reinforcing steel (both in tension and compression) is  $0.002 + (0.87f_y/E_s)$  (again, in general, can be any value recommended by corresponding design standard); and
- v. Design strength of section is reached when either/both of the following happens:
  - a) Highly compressed concrete edge reaches limiting strain of concrete (0.0035),
  - b) Outermost layer of reinforcing steel in tension reaches limiting strain of reinforcing steel ( $0.002 + 0.87f_y/E_s$ ).

### 2.2 Material constitutive relations

The design compressive stress-strain curves of constituent materials are recommended in design codes. Here, the Indian Standard Code of Practice for Plain and Reinforced Concrete is referred to demonstrate the use of above methodology, both for reinforcing steel and concrete (Fig.1) [12, 1]. Accordingly, the design compressive strength of concrete is assumed to be 45% of the characteristic standard cube strength  $f_{ck}$ . The ascending part of the curve is represented by second-degree parabola up to compressive strain of 0.002 [13], with uniform stress post-peak branch up to strain of 0.0035. Thus, the compressive stress  $f_c$  in concrete corresponding to compressive strain  $\epsilon_c$  is:

$$f_c = \begin{cases} 0.45f_{ck} \left[ \left( \frac{2\epsilon_c}{0.002} \right) - \left( \frac{\epsilon_c}{0.002} \right)^2 \right] & \text{for } 0 \leq \epsilon_c \leq 0.002 \\ 0.45f_{ck} & \text{for } 0.002 < \epsilon_c \leq 0.0035 \end{cases} \quad (1)$$

Thus, the average compressive stress  $f_{c,avg}$  in concrete for given strain ( $\epsilon_c$ ) at the highly compressed edge and the distance  $\bar{y}$  of resultant compressive force in concrete from the neutral axis are:

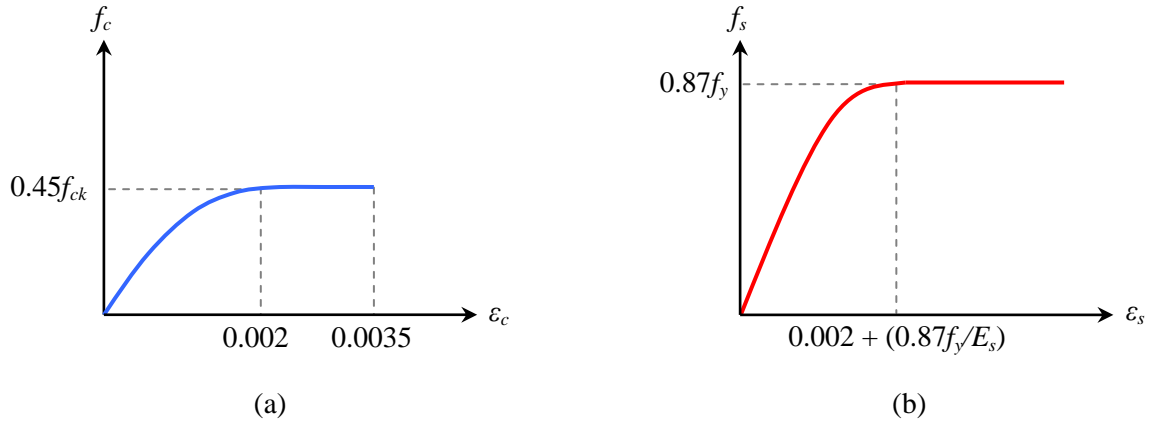


Fig. 1 – Design stress-strain relationship of (a) concrete (b) steel

$$f_{c,avg} = \begin{cases} 0.45f_{ck} \left[ \left( \frac{\varepsilon_c}{0.002} \right) - \frac{1}{3} \left( \frac{\varepsilon_c}{0.002} \right)^2 \right] & \text{for } 0 \leq \varepsilon_c \leq 0.002 \\ 0.45f_{ck} \left[ 1 - \frac{1}{3} \left( \frac{0.002}{\varepsilon_c} \right) \right] & \text{for } 0.002 < \varepsilon_c \leq 0.0035 \end{cases}, \text{ and} \quad (2)$$

$$\bar{y} = \begin{cases} \left[ \frac{2}{3} - \frac{1}{4} \left( \frac{\varepsilon_c}{0.002} \right) \right] x_u & \text{for } 0 \leq \varepsilon_c \leq 0.002 \\ \left[ \frac{1}{2} - \frac{1}{12} \left( \frac{0.002}{\varepsilon_c} \right)^2 \right] x_u & \text{for } 0.002 < \varepsilon_c \leq 0.0035 \end{cases} \quad (3)$$

### 2.3 Equations of equilibrium

Using the methodology, assumptions and material constitutive relations, axial force  $P$  and bending moment  $M$  capacities at select points on the interaction diagram are determined using two basic equations of equilibrium namely,

- 1)  $\sum F_y = 0$ , to obtain design axial force  $P$ , and
- 2)  $\sum M = 0$ , to obtain design bending moment  $M$ , estimated about GCA of the section for the given level of axial load  $P$ .

### 2.4 Characterization of discrete points on $P$ - $M$ interaction curve

Typical  $P$ - $M$  interaction curve for I shape wall is shown in Figure 2. Salient points used to obtain the interaction curve are marked along with respective strain and stress profiles, and are described below:

Point A: It represents state of pure axial compression. Entire cross section of wall is subjected to uniform compressive strain of 0.0035. Failure of section is governed by crushing of concrete.

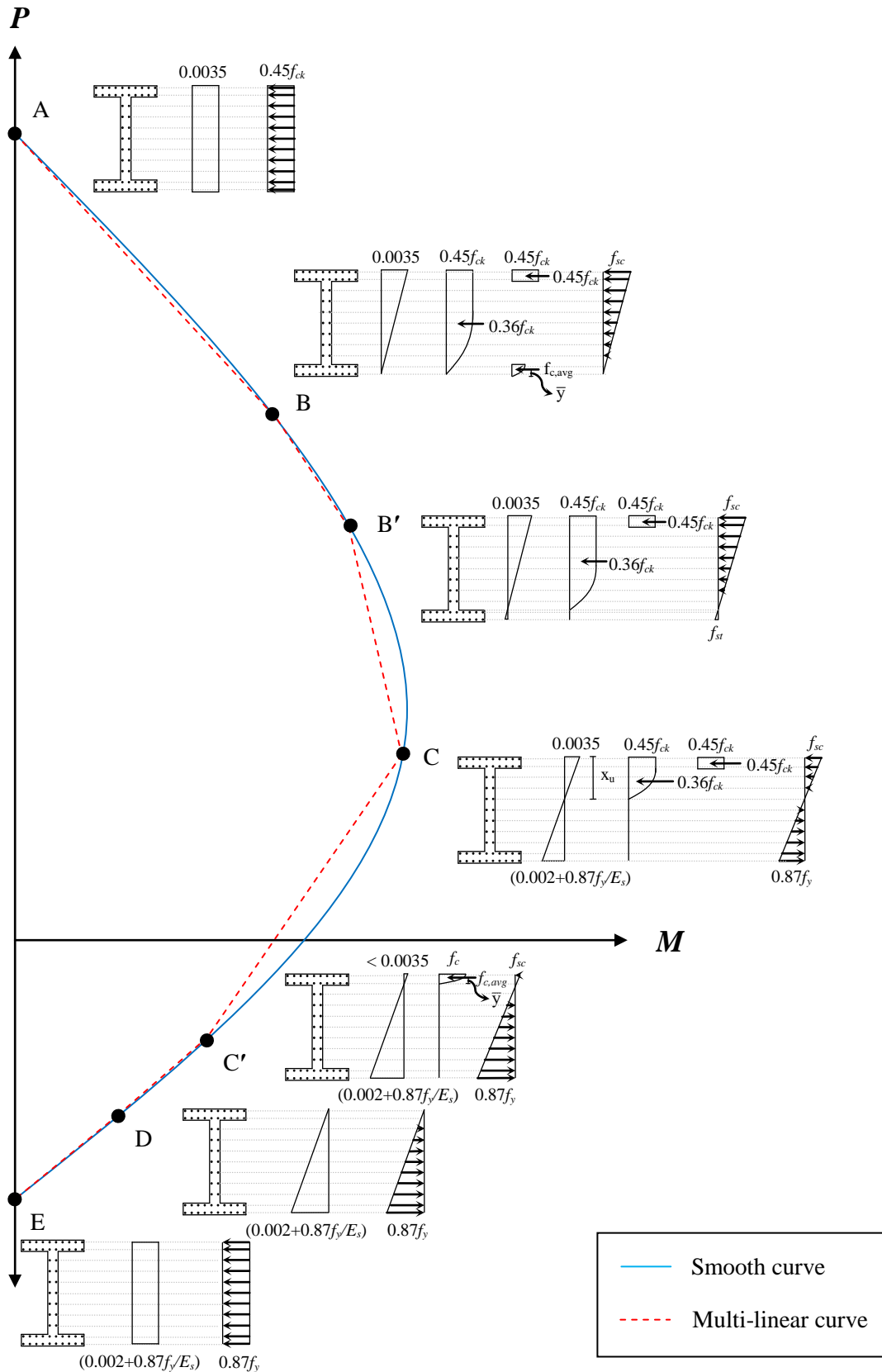


Fig. 2 – Typical  $P$ - $M$  interaction curve for I-shape RC wall with stress and strain profiles at select points

Point B: At this point on the interaction curve, the highly compressed (top) concrete edge is at strain of 0.0035, linearly decreasing to zero at the other (bottom) concrete edge. Thus, depth of neutral axis is same as length of wall. Failure of section is governed by crushing of concrete.

Point B': In case of flanged walls, this point represents a state where strain in concrete at intersection of web and bottom tension flange is zero, while the highly compressed concrete edge remains at a strain of 0.0035.

Point C: This point represents balanced failure condition. Here, the strain at the highly compressed concrete edge is equal to limiting compressive strain of concrete in compression, *i.e.*, 0.0035, and the strain in outermost reinforcing steel layer in tension is equal to limiting tensile strain in steel, *i.e.*,  $(0.002+0.87f_y/E_s)$ , simultaneously.

Point C': In case of flanged walls, this point represents a state where strain in concrete at intersection of web and top compression flange is zero while outermost reinforcing steel layer remains at a strain of  $(0.002+0.87f_y/E_s)$ . Depth of neutral axis is equal to thickness of flange.

Point D: At this point, strain at topmost concrete layer is zero while tensile strain in bottommost reinforcing steel layer is  $(0.002+0.87f_y/E_s)$ . Thus, neutral axis depth is zero. From this point onwards, entire wall section is under tension.

Point E: This point represents state of pure axial tension. Strain in both topmost and bottommost reinforcing steel layers is  $(0.002+0.87f_y/E_s)$ . As per third assumption, whole section is under uniform design tensile stress of  $0.87f_y$ .

### 3. Expressions of design $P$ and $M$

The use of the proposed methodology is demonstrated using five commonly used cross-sections of RC structural walls (Fig.3). Closed form equations of  $P$  and  $M$  at the select points on the respective design interaction diagram are given below.

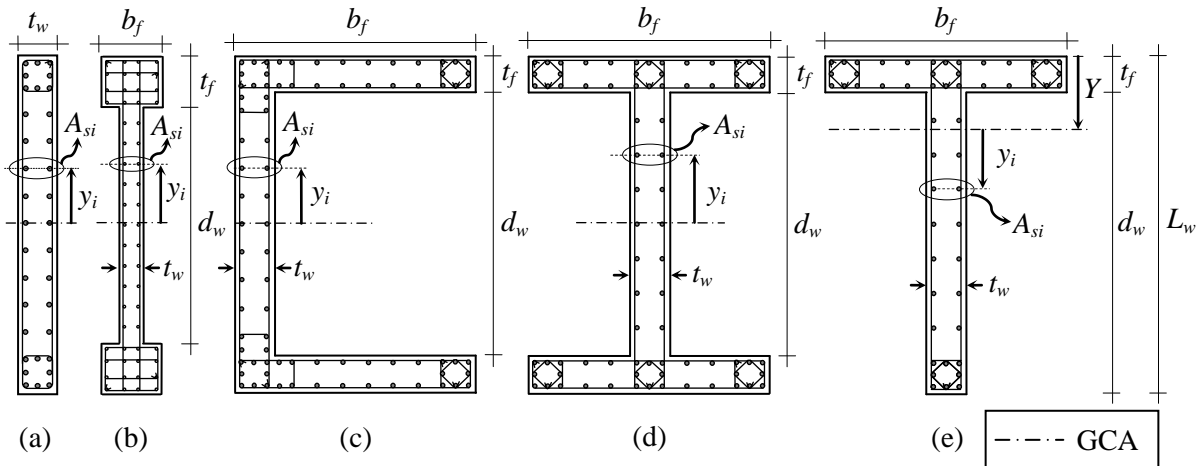


Fig. 3 – Cross section of (a) Rectangular (b) Dumbbell (c) C-shape (d) I-shape (e) T-shape RC wall

#### 3.1 Rectangular wall sections (with and without embedded boundary elements)

**Point A**

$$P = 0.45f_{ck} L_w t_w + \sum_{i=1}^n (f_{sc,i} - 0.45f_{ck}) A_{sc,i} \quad (4)$$

$$M = 0$$

**Point B**

$$P = 0.36f_{ck} L_w t_w + \sum_{i=1}^n (f_{sc,i} - f_{csc,i}) A_{sc,i}$$



$$M = 0.36f_{ck} L_w t_w \left( \frac{L_w}{2} - 0.42L_w \right) + \sum_{i=1}^n (f_{sc,i} - f_{csc,i}) A_{sc,i} y_i \quad (5)$$

**Point C**

$$P = 0.36f_{ck} x_u t_w + \sum_{i=1}^n (f_{sc,i} - f_{csc,i}) A_{sc,i} - \sum_{j=1}^m f_{st,j} A_{st,j} \quad (6)$$

$$M = 0.36f_{ck} x_u t_w \left[ \frac{L_w}{2} - 0.42x_u \right] + \sum_{i=1}^n (f_{sc,i} - f_{csc,i}) A_{sc,i} y_i + \sum_{j=1}^m f_{st,j} A_{st,j} y_j$$

where,

$$x_u = (L_w - d') \left[ \frac{0.0035}{0.0055 + \frac{0.87f_y}{E_s}} \right]$$

**Point D**

$$P = -\sum_{j=1}^m f_{st,j} A_{st,j} \quad (7)$$

$$M = \sum_{j=1}^m f_{st,j} A_{st,j} y_j$$

**Point E**

$$P = -0.87f_y \sum_{j=1}^m A_{st,j} \quad (8)$$

$$M = 0$$

### 3.2 I, C, Dumbbell shape wall sections

$P$ - $M$  interaction envelope for a section is function of cross sectional dimension, material properties and distribution of reinforcement across bending axis. Thus, for RC wall of I and C shape (bending about major axis), same expressions of design  $P$  and  $M$  can be used. Also, due to similarity in shape, following expressions of design  $P$  and  $M$  for I-shape wall also apply to dumbbell shape wall.

**Point A**

$$P = 0.45f_{ck} [L_w t_w + 2t_f (b_f - t_w)] + \sum_{i=1}^n (f_{sc,i} - 0.45f_{ck}) A_{sc,i} \quad (9)$$

$$M = 0$$

**Point B**

$$P = 0.36f_{ck} L_w t_w + 0.45f_{ck} t_f (b_f - t_w) + f_{c,avg} t_f (b_f - t_w) + \sum_{i=1}^n (f_{sc,i} - f_{csc,i}) A_{sc,i}$$

$$M = 0.36f_{ck} L_w t_w \left( \frac{L_w}{2} - 0.42L_w \right) + 0.45f_{ck} t_f (b_f - t_w) \left( \frac{L_w}{2} - \frac{t_f}{2} \right) - f_{c,avg} t_f (b_f - t_w) \left( \frac{L_w}{2} - \bar{y} \right) + \sum_{i=1}^n (f_{sc,i} - f_{csc,i}) A_{sc,i} y_i \quad (10)$$



#### Point B'

$$\begin{aligned}
 P &= 0.36f_{ck}(L_w - t_f)t_w + 0.45f_{ck}t_f(b_f - t_w) + \sum_{i=1}^n (f_{sc,i} - f_{csc,i})A_{sc,i} - \sum_{j=1}^m f_{st,j}A_{st,j} \\
 M &= 0.36f_{ck}(L_w - t_f)t_w \left[ \frac{L_w}{2} - 0.42(L_w - t_f) \right] + 0.45f_{ck}t_f(b_f - t_w) \left( \frac{L_w}{2} - \frac{t_f}{2} \right) \\
 &\quad + \sum_{i=1}^n (f_{sc,i} - f_{csc,i})A_{sc,i}y_i + \sum_{j=1}^m f_{st,j}A_{st,j}y_j
 \end{aligned} \tag{11}$$

#### Point C

$$\begin{aligned}
 P &= 0.36f_{ck}x_u t_w + 0.45f_{ck}t_f(b_f - t_w) + \sum_{i=1}^n (f_{sc,i} - f_{csc,i})A_{sc,i} - \sum_{j=1}^m f_{st,j}A_{st,j} \\
 M &= 0.36f_{ck}x_u t_w \left[ \frac{L_w}{2} - 0.42x_u \right] + 0.45f_{ck}t_f(b_f - t_w) \left( \frac{L_w}{2} - \frac{t_f}{2} \right) \\
 &\quad + \sum_{i=1}^n (f_{sc,i} - f_{csc,i})A_{sc,i}y_i + \sum_{j=1}^m f_{st,j}A_{st,j}y_j
 \end{aligned} \tag{12}$$

#### Point C'

$$\begin{aligned}
 P &= f_{c,avg}b_f t_f + \sum_{i=1}^n (f_{sc,i} - f_{csc,i})A_{sc,i} - \sum_{j=1}^m f_{st,j}A_{st,j} \\
 M &= f_{c,avg}b_f t_f \left[ \frac{L_w}{2} - (t_f - \bar{y}) \right] + \sum_{i=1}^n (f_{sc,i} - f_{csc,i})A_{sc,i}y_i + \sum_{j=1}^m f_{st,j}A_{st,j}y_j
 \end{aligned} \tag{13}$$

#### Point D

$$\begin{aligned}
 P &= -\sum_{j=1}^m f_{st,j}A_{st,j} \\
 M &= \sum_{j=1}^m f_{st,j}A_{st,j}y_j
 \end{aligned} \tag{14}$$

#### Point E

$$\begin{aligned}
 P &= -0.87f_y \sum_{j=1}^m A_{st,j} \\
 M &= 0
 \end{aligned} \tag{15}$$

### 3.3 T-shape wall sections

T-shape wall is asymmetric about major axis of bending, and hence, it is possible to develop two different  $P$ - $M$  interaction curves for bending about the same major axis, depending on whether the flange is in compression or tension, during pure bending condition.

#### 3.3.1 Flange in compression

##### Point A

$$\begin{aligned}
 P &= 0.45f_{ck} \left[ L_w t_w + t_f(b_f - t_w) \right] + \sum_{i=1}^n (f_{sc,i} - 0.45f_{ck})A_{sc,i} \\
 M &= 0
 \end{aligned} \tag{16}$$



**Point B**

$$P = 0.36f_{ck}L_w t_w + 0.45f_{ck}t_f(b_f - t_w) + \sum_{i=1}^n (f_{sc,i} - f_{csc,i})A_{sc,i} \quad (17)$$

$$M = 0.36f_{ck}L_w t_w(Y - 0.42L_w) + 0.45f_{ck}t_f(b_f - t_w)\left(Y - \frac{t_f}{2}\right) + \sum_{i=1}^n (f_{sc,i} - f_{csc,i})A_{sc,i}y_i$$

**Point C**

$$P = 0.36f_{ck}x_u t_w + 0.45f_{ck}t_f(b_f - t_w) + \sum_{i=1}^n (f_{sc,i} - f_{csc,i})A_{sc,i} - \sum_{j=1}^m f_{st,j}A_{st,j}$$

$$M = 0.36f_{ck}x_u t_w(Y - 0.42x_u) + 0.45f_{ck}t_f(b_f - t_w)\left(Y - \frac{t_f}{2}\right) + \sum_{i=1}^n (f_{sc,i} - f_{csc,i})A_{sc,i}y_i \quad (18)$$

$$+ \sum_{j=1}^m f_{st,j}A_{st,j}y_j$$

**Point C'**

$$P = f_{c,avg}b_f t_f + \sum_{i=1}^n (f_{sc,i} - f_{csc,i})A_{sc,i} - \sum_{j=1}^m f_{st,j}A_{st,j} \quad (19)$$

$$M = f_{c,avg}b_f t_f[Y - (t_f - \bar{y})] + \sum_{i=1}^n (f_{sc,i} - f_{csc,i})A_{sc,i}y_i + \sum_{j=1}^m f_{st,j}A_{st,j}y_j$$

**Point D**

$$P = -\sum_{j=1}^m f_{st,j}A_{st,j} \quad (20)$$

$$M = \sum_{j=1}^m f_{st,j}A_{st,j}y_j$$

**Point E**

$$P = -0.87f_y \sum_{j=1}^m A_{st,j} \quad (21)$$

$$M = 0$$

**3.3.2 Flange in tension**

**Point A**

$$P = 0.45f_{ck}[L_w t_w + t_f(b_f - t_w)] + \sum_{i=1}^n (f_{sc,i} - 0.45f_{ck})A_{sc,i} \quad (22)$$

$$M = 0$$

**Point B**

$$P = 0.36f_{ck}L_w t_w + f_{c,avg}t_f(b_f - t_w) + \sum_{i=1}^n (f_{sc,i} - f_{csc,i})A_{sc,i} \quad (23)$$

$$M = 0.36f_{ck}L_w t_w(Y - 0.42L_w) + f_{c,avg}t_f(b_f - t_w)[Y - (L_w - \bar{y})] + \sum_{i=1}^n (f_{sc,i} - f_{csc,i})A_{sc,i}y_i$$



#### Point B'

$$P = 0.36f_{ck}d_w t_w + \sum_{i=1}^n (f_{sc,i} - f_{csc,i})A_{sc,i} - \sum_{j=1}^m f_{st,j}A_{st,j} \quad (24)$$

$$M = 0.36f_{ck}d_w t_w (Y - 0.42d_w) + \sum_{i=1}^n (f_{sc,i} - f_{csc,i})A_{sc,i}y_i + \sum_{j=1}^m f_{st,j}A_{st,j}y_j$$

#### Point C

$$P = 0.36f_{ck}x_u t_w + \sum_{i=1}^n (f_{sc,i} - f_{csc,i})A_{sc,i} - \sum_{j=1}^m f_{st,j}A_{st,j} \quad (25)$$

$$M = 0.36f_{ck}x_u t_w (Y - 0.42x_u) + \sum_{i=1}^n (f_{sc,i} - f_{csc,i})A_{sc,i}y_i + \sum_{j=1}^m f_{st,j}A_{st,j}y_j$$

#### Point D

$$P = -\sum_{j=1}^m f_{st,j}A_{st,j} \quad (26)$$

$$M = \sum_{j=1}^m f_{st,j}A_{st,j}y_j$$

#### Point E

$$P = -0.87f_y \sum_{j=1}^m A_{st,j} \quad (27)$$

$$M = 0$$

## 4. Numerical study

### 4.1 Modeling

Numerical models of RC walls of rectangular, dumbbell, I, C and T shapes are developed in PERFORM-3D [14]. These walls, each of 45 m height, are modeled as vertical cantilevers with full fixity at base using 4-noded 'shear wall elements' that uses fiber sections. Typical optimization of fiber sizes is carried out in all cases. One of such fiber section used for rectangular wall is shown in Figure 4. The section consists of 8 identical concrete fibers of size  $625 \times 250 \text{ mm}^2$  and 8 steel fibers of area  $1885 \text{ mm}^2$  each. Material properties for M25 grade of concrete and Fe415 grade of reinforcing steel are used in this study. Constitutive models for concrete and reinforcing steel defined in section 2.2, are approximated by trilinear curves as input. Cross-section dimensions and reinforcement details of each wall are given in Table 1. Pushover analysis is performed of each wall for varying levels of axial loads. To comply with fifth assumption in section 2.1, two limit states are defined, (i) limiting compressive strain of 0.0035 at highly compressed concrete edge and, (ii) limiting tensile strain of 0.0038 in reinforcing steel (of yield strength of 415 MPa). Analysis is stopped when either of the two limit states is reached.

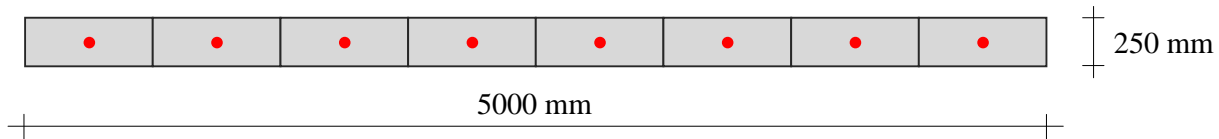


Fig. 4 – Fiber section for RC rectangular wall

Table 1 – Cross-sectional details of RC walls

Wall shape in plan	$L_w$	Web		Flange		Reinforcement	
		$d_w$	$t_w$	$b_f$	$t_f$	Web	Flange
Rectangular	5000	5000	250	-	-	48 Y20 in 2 layers	-
Dumbbell	5000	3600	250	700	700	48 Y20 in 2 layers	16 Y20 in 4 layers
I & C	5000	4500	250	5000	250	48 Y20 in 2 layers	48 Y20 in 2 layers
T	5000	4750	250	5000	250	48 Y20 in 2 layers	48 Y20 in 2 layers

(All dimensions are in mm)

## 4.2 Analysis results

Maximum base shear induced in wall is extracted from pushover analysis results. This base shear is then multiplied by the height of wall to obtain maximum moment ( $M$ ) mobilized at base of the wall, for a given axial load ( $P$ ). Thus, coordinates ( $M$ ,  $P$ ) of points on  $P$ - $M$  interaction diagram are numerically obtained to draw a smooth strength envelope curve. Normalized values of  $P$  ( $P_N = P/f_{ck}t_wL_w$ ) and  $M$  ( $M_N = M/f_{ck}t_wL_w^2$ ) obtained by this method for different wall sections (Table 1), are listed in Table 2.

Table 2 – Normalized values of  $P$  and  $M$  obtained from numerical analysis

Rectangular wall		Dumbbell shape wall		I shape wall		C shape wall		T shape wall			
								Flange in Tension ( $T_{TF}$ )		Flange in Compression ( $T_{CF}$ )	
$P_N$	$M_N$	$P_N$	$M_N$	$P_N$	$M_N$	$P_N$	$M_N$	$P_N$	$M_N$	$P_N$	$M_N$
0.62	0	0.96	0	1.84	0	1.84	0	1.22	0	1.22	0
0.53	0.03	0.82	0.05	1.58	0.12	1.58	0.12	1.04	0.04	1.04	0.11
0.44	0.06	0.69	0.10	1.31	0.24	1.31	0.24	0.87	0.08	0.87	0.18
0.35	0.08	0.55	0.14	1.05	0.35	1.05	0.35	0.69	0.12	0.69	0.21
0.27	0.09	0.41	0.17	0.79	0.44	0.79	0.44	0.52	0.15	0.52	0.19
0.18	0.09	0.27	0.17	0.53	0.45	0.53	0.45	0.35	0.18	0.35	0.15
0.09	0.08	0.14	0.15	0.26	0.35	0.26	0.35	0.17	0.20	0.17	0.12
0	0.06	0	0.11	0	0.24	0	0.24	0	0.17	0	0.08
-0.06	0.04	-0.10	0.07	-0.17	0.16	-0.17	0.16	-0.12	0.13	-0.12	0.05
-0.12	0.02	-0.19	0.03	-0.35	0.08	-0.35	0.08	-0.23	0.07	-0.23	0.02
-0.17	0	-0.29	0.00	-0.52	0	-0.52	0	-0.35	0	-0.35	0

## 4.3 Comparison of results of proposed method with numerical results

Design  $P$ - $M$  interaction diagrams, of different RC wall sections determined using the proposed methodology, are compared with the numerical results (Fig. 5). In general, proposed method gives reasonably good results. Thus, the proposed method can conveniently be used in routine design; maximum difference of about 11% is observed in estimates of flexural strength at higher levels of axial load, due to limited number of points considered in the proposed method.

## 5. Summary and conclusion

A strain-based procedure is proposed to obtain design  $P$ - $M$  interaction curves of RC wall sections of different shapes. Proposed method includes expressions with basic arithmetic operations that can be solved manually or using simple spread sheets. The procedure is simple, non-iterative and efficient, enabling it to be used in design offices or at construction sites to make quick judgment on adequacy of wall sections.

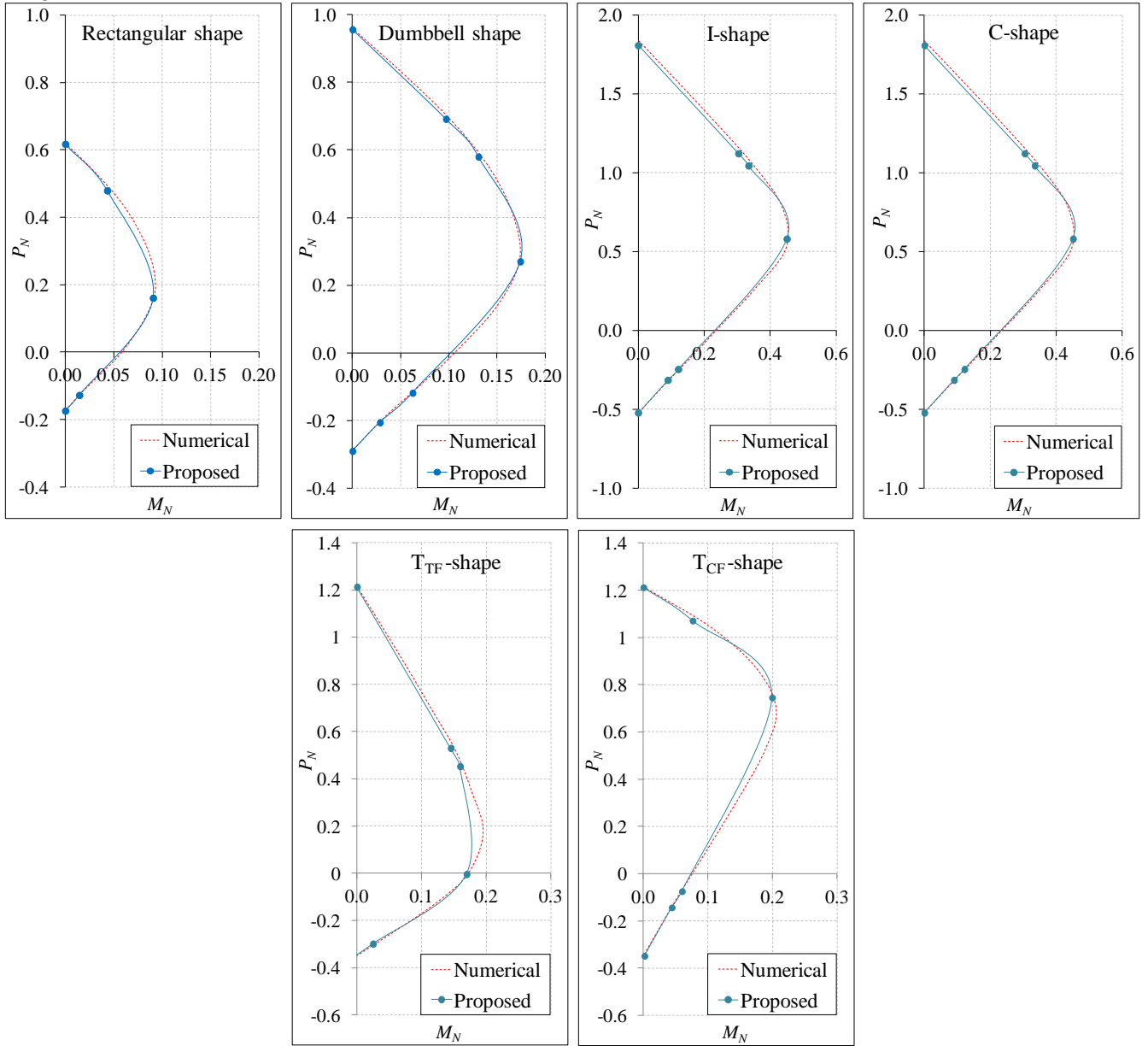


Fig. 5 – Normalized  $P$ - $M$  interaction curves for RC wall sections

## 6. Symbols

$A_{sc,i}$	:	Area of reinforcing steel in compression in $i^{\text{th}}$ layer
$A_{st,j}$	:	Area of reinforcing steel in tension in $j^{\text{th}}$ layer
$b_f$	:	Effective width of flange
$d'$	:	Effective cover
$d_w$	:	Depth of web of flanged wall
$E_s$	:	Young's modulus for steel
$f_{ck}$	:	Characteristic compressive strength of concrete
$f_{c,avg}$	:	Average compressive stress in concrete in compression
$f_{csc}$	:	Compressive stress in concrete at the level of reinforcing steel in compression
$f_{sc}$	:	Stress in reinforcing steel in compression
$f_{st}$	:	Stress in reinforcing steel in tension
$f_y$	:	Yield strength of steel



GCA	:	Geometric centroidal axis
$m$	:	Total number of layers of steel bars in tension
$n$	:	Total number of layers of steel bars in compression
$L_w$	:	Length of wall
$t_f$	:	Thickness of flange of flanged wall
$t_w$	:	Thickness of rectangular wall or web thickness of flanged wall
$Y$	:	Depth of GCA from topmost concrete edge
$y_i$	:	Distance of $i^{\text{th}}$ steel layer from GCA
$\bar{y}$	:	Distance between centroid of concrete stress block and neutral axis

## 7. References

- [1] SP16: 1980 (1980): *Design Aids for Reinforced Concrete to IS 456: 1978*, Bureau of Indian Standards, New Delhi.
- [2] ACI SP-17(14) (2015): *The reinforced concrete design handbook*, American Concrete Institute, Farmington Hills, MI, **03**.
- [3] ACI 318-83 (1983): *Building Code Requirements for Reinforced Concrete*, American Concrete Institute, Detroit.
- [4] IS13920:1993 (2003): *Indian Standard Code Of Practice for Ductile Detailing Of Reinforced Concrete Structures Subjected To Seismic Forces*, Bureau of Indian Standards, New Delhi.
- [5] ACI 318-14 (2015): *Building Code Requirements for Structural Concrete*, American Concrete Institute, Farmington Hills, MI.
- [6] NZS 3101 (2006): *Concrete Structures Standard – Part 1: The Design of Concrete Structures*, Standards New Zealand, Wellington.
- [7] Eurocode 8 (2004): *Design of structures for earthquake resistance – Part 1: General rules, seismic actions and rules for buildings*, European Committee for Standardization, Brussels.
- [8] Medhekar MS, Jain AK (1993): Seismic behavior, design and detailing of RC shear walls, Part I: Behavior and strength. *The Indian Concrete Journal*, July 1993, **67** (07), 311-318.
- [9] Narahari P, Dasgupta K. (2011): Axial force bending moment interaction of earthquake resistant reinforced concrete flanged structural walls. *International Journal of Earth Sciences and Engineering*, **04** (06), 554-559.
- [10] Dabiri H, Kavyani A, Kheyroddin A (2014): Axial force-moment interaction diagrams to calculate shear wall reinforcement. *Trends In Life Sciences*, **03** (03), 561-570.
- [11] Majeed AZ, Goswami R, Murty CVR (2015): Mechanics-driven hand calculation approach for obtaining design P-M interaction curves of RC sections. *The Indian Concrete Journal*, September 2015, **89** (9), 59-68.
- [12] IS456: 2000 (2000): *Indian Standard Code of Practice for Plain and Reinforced Concrete*, Bureau of Indian Standards, New Delhi.
- [13] Kent DC, Park R (1971): Flexural members with confined concrete. *Journal of the Structural Division, ASCE*, **97** (07), 1969-90.
- [14] CSI Perform 3D V5. (2011): *Nonlinear Analysis and Performance Assessment for 3D Structures*, Computer and Structures, Inc. Berkeley, CA.